A comprehensive study of the impact of electrode design and iron deposition mechanism on the enhancement of the capacity of an all-iron redox flow battery (AIFB) has been conducted. The research is focused on revealing the complex interaction between electrode architecture, iron deposition behaviour, and battery capacity.

Using a developed experimental setup, five different electrode designs are investigated. These designs include variations in the arrangement of carbon felt (CF) and non-woven fabric (NWF) layers and critical factors affecting iron deposition. Battery charge and discharge experiments were carried out under controlled conditions, simulating practical operating regimes with a current density of 50 mA/cm^2 and a compression ratio of 80 %.

The results demonstrate the influence of electrode design on iron deposition and, consequently, on battery capacity. The electrode configuration with two layers of CF and two layers of NWF exhibits a specific capacity exceeding 700 mA•h/cm^2.

Analysis using scanning electron microscopy (SEM) complements the capacity determination results by providing valuable information about the spatial distribution of iron on the electrode surfaces. Furthermore, quantitative analysis using ZAF correction reveals uniform models of iron deposition on the surface of electrode E, indicating its potential for optimizing AIFB performance.

This study provides a comprehensive understanding of the relationship between electrode design, iron deposition behaviour, and AIFB capacity. The results offer insights for improving electrode configurations, ultimately contributing to the development of efficient energy storage solutions

Keywords: all-iron flow battery, electrode architecture, iron deposition, battery capacity, carbon felt

UDC 621.3.035.221.15
DOI: 10.15587/1729-4061.2023.288452

DEVISING OF A METHOD FOR IMPROVING ANODE CAPACITY FOR AN ALL-IRON FLOW BATTERY

Andrii Bondar
Corresponding author
Postgraduate Student*
E-mail: parkawaymc@gmail.com
Olga Linyucheva
Doctor of Technical Sciences, Professor, Dean*
Mykhaylo Byk
PhD, Associate Professor*
*Department of Electrochemical Productions Technology
National Technical University of Ukraine
"Igor Sikorsky Kyiv Polytechnic Institute"
Beresteiskyi ave., 37, Kyiv, Ukraine, 03056

Received date 18.07.2023
Accepted date 26.09.2023
Published date 30.10.2023

How to Cite: *Bondar, A., Linyucheva, O., Byk, M. (2023). Devising of a method for improving anode capacity for an all-iron flow battery. Eastern-European Journal of Enterprise Technologies, 5 (6 (125)), 49–57. doi: https://doi.org/10.15587/1729-4061.2023.288452*

1. Introduction

Starting from 2010, a significant increase in the installed capacity of wind and solar power plants has been observed, which is supported by political and social imperative for the transition to renewable energy generation. Regardless, the contribution of energy to carbon dioxide emissions accounts for 55 %, which forces initiatives to be taken to change the volume and absolute amount of carbon dioxide emissions [1, 2]. By increasing the amount of unpredictable generation of renewable energy, it is necessary to increase the amount of flexible electricity generation, which can be used to balance the power in the power grid. In this regard, there is a need to design a tool for the long-duration accumulation of "green" electricity, which could increase the predictability of renewable energy production and act as a flexible generation [3]. Owing to such an advancement, society will be able to increase the number of solar and wind power plants without parallel deployment of coal generation.

Promising candidates for medium (hours and days) and long-term (weeks and months) accumulation can be:

– hydro-accumulating power plants;
– hydrogen production and conversion technologies;
– mechanical (gravity) energy storage;
– compressed air storage technologies;
– redox flow batteries.

Redox flow batteries have relatively high efficiency and independence from the landscape, compared to other technologies. Among the various types of flow batteries, the most researched and developed are batteries based on the following pairs of chemical elements [4–8]: V/V; Zn/O_2; Zn/Br_2; H_2/Br_2; Fe/Cr; Fe/Fe; Zn/Ce.

The main materials for the production of all-iron flow batteries are iron chloride, sodium chloride, and graphite felt. Considering the availability of these components, the research and development of industrial storage systems of all-iron flow batteries based on redox pair Fe^{2+}/Fe^{3+} are promising.

2. Literature review and problem statement

In one of the first works [9] addressing the all-iron flow batteries (AIFB), a viable solution for storing energy obtained, for example, as a result of the operation of a solar power plant, etc., is reported. The basis of such a flow battery is an aqueous electrolyte solution, which consists of an iron salt such as $FeCl_2$ or $FeSO_4$ and an inert auxiliary salt such as NH_4Cl or NaCl. The battery charge cycle involves the reduction of ferrous ions with a water-based chloride electrolyte at the negative electrode, while the positive electrode oxidizes ferrous ions (2) to ferrous ions (3). The negative electrode consists of a solid graphite or titanium plate, while a material with a high specific area was used for the positive electrode. Thus, experiments were conducted using one cell with an area of 100 cm^2 with a microporous plastic separator

operating at a current density of 60 mA/cm^2 and a temperature of 60 °C. The cell demonstrated energy storage and discharge capabilities, achieving a current efficiency of 90 % and a round-trip efficiency of 50 %, indicating the loss of half of the battery capacity. In addition, the cell demonstrated a maximum discharge power density of 50 mW/cm^2. It should be noted that today these results need to be improved, given the economic disadvantage, and the battery configuration needs to be modified.

When charging AIFB, Fe^{2+} ions are oxidized to Fe^{3+} ions on the positive electrode. At the same time, the reduction of ferrous ions with the precipitation of metallic iron occurs at the negative electrode. During battery discharge, these processes occur in the opposite way: metallic iron is oxidized and dissolves again in the electrolyte at the negative electrode, while iron ions (3) are reduced to ferrous ions at the positive electrode, which is a key process in the operation of the battery. Therefore, understanding the factors that can affect it could solve the problem of improving the effectiveness of AIFB.

For example, in works [10–12], it was found that the main drawback of the all-iron flow battery is the side process of hydrogen evolution (HER – hydrogen evolution reaction), which occurs on the negative electrode during battery charging and discharging. Thus, under the charge mode, there will also be a decrease in the concentration of H^+ ions (H_3O^+) at the negative electrode, where gaseous H_2 is formed during the hydrogen evolution reaction. An option to overcome this drawback is to optimize the current density over the entire surface of the electrode, which will increase the overvoltage of hydrogen release compared to the overvoltage of iron release.

Another serious problem of AIFB is the limited capacity of the negative electrode [13, 14]. Since iron is deposited on the anode during battery charging, there must be enough space in the anode chamber to accommodate the deposited iron. Otherwise, there will not be enough volume for electrolyte circulation, which will complicate the operation of the battery. Since the AIFB is designed for long-duration energy storage (typically 6 to 20 hours), it is very important to be sure that the negative electrode capacity is sufficient for such use cases. Thus, it is important to study the maximum capacity of various structures of the negative electrode.

Therefore, the release of hydrogen and the formation of metal dendrites at high current densities are the biggest problems of AIFB; attempts were made to take them into account in later works.

In [10], a recombination element (regenerative cell) was tested during the operation of AIFB in order to prevent the irreversible loss of capacity caused by the formation of hydrogen during 100 two-hour charge/discharge cycles. In addition, experiments were performed to regenerate the electrolyte with external hydrogen to reverse the irreversible losses, and different substrate materials for iron deposition were investigated, such as Kynol cloth, and different microporous and ion exchange membranes (Nafion, Fumatech FAP-450) were used. All the listed modernization methods made it possible to reach the value of energy efficiency of 70 % at 12.5 mA·cm^{-2}, 47 mW·cm^{-2}, and specific power of 75 mA·cm^{-2}, which is quite high, but requires further improvement.

Study [11] that considered achieving the maximum coating capacity for various electrode designs led to promising results with 145 mA·h/cm^2 for a copper coating. However, given the desired operating conditions of 50 mA/cm^2 and a discharge duration of 6–20 hours, a coating capacity of 145 mA·h/cm^2 is insufficient.

Paper [15] highlighted the main specifications for electrodes in AIFB, including high specific surface area, electrochemical activity, electronic conductivity, economic efficiency, and corrosion resistance. Carbon fiber-based materials such as carbon paper (CP), graphite felt (GF), and carbon felt (CF) are well suited for use as electrode materials due to their favorable properties. In turn, the achievement of high liquid permeability in the structure of an AIFB electrode is of crucial importance for increasing the efficiency of the battery.

Thus, it is clear that there is a need to research and develop new approaches to further increase the coating capacity. This is due to the fact that there is a clear problem of developing an anode with a capacity that satisfies the need for 600 mA-h/cm^2, which is associated with the limited area of iron deposition by the conductive carrier, the complexity of the nature of iron deposition on the conductive material, and the ingrowth of iron into the membrane with subsequent cell shorting.

3. The aim and objectives of the study

The purpose of this work is to devise a method of increasing the capacity of various designs of the anode of an all-iron flow battery. This method is considered as a part of the strategy for the realization of an electrochemical storage of electrical energy with a long-term capacity. From a practical point of view, the identified characteristics of the anode of the battery could allow determining the optimal design of the electrode with a high capacity in the production technology of the all-iron flow rechargeable battery. This constitutes the prerequisites for the transfer of the obtained technological solutions to the development of industrial energy storage systems of high capacity and efficiency.

To achieve the goal of the study, the following tasks were solved:

– to investigate the differences in capacity between different anode designs and find out the factors affecting the capacity of batteries;

– to analyze the distribution of deposited iron on the surface of the electrodes;

– to investigate the distribution of iron deposition using scanning electron microscopy and quantitative analysis using the ZAF correction method.

4. The study materials and methods

4. 1. The object and hypothesis of the study

The object of our research is the design of the anode of an all-iron flow battery, which includes a combination of carbon materials and their configuration with non-conductive felt. The research is aimed at studying the relationship between the design of anodes, their microstructure, features of iron deposition, and the capacity of anode materials.

The main hypothesis of the study assumes that by changing the design of the anode, its capacity can be improved by increasing the amount of free volume between the anode and the membrane for the deposition of iron as an active substance.

The research was conducted assuming that a current density of 50 mA/cm^2 is optimal for achieving economic

goals and target voltaic efficiency. In addition, the study was carried out at a compression ratio of the anode material of 80 %, which, from the previous works, is optimal for achieving high voltaic efficiency and anode capacity.

4. 2. Materials and reagents

All reagents were of pure chemical quality, and all electrolytes were prepared using deionized water.

For experiments with AIFB, carbon felt (CF) from SGL Carbon with a thickness of 2.5 mm was obtained. All carbon felt materials were pre-treated with nitric acid to improve wettability. The felt was soaked in 1 M HNO_3 for one hour and then rinsed with deionized water until the pH of the wash water reached 6. The non-conductive (non-electric-conductive) felt (NCF) used was a 1 mm thick polyester felt. Daramic membrane material (175 SLI Flatsheet Membrane) 220 mm thick was obtained from Daramic (Charlotte, NC). Nafion 115 (Proton Power, Lenoir City, TN) was also used as a membrane.

4. 3. Scanning electron microscopy (SEM) and study of the microstructure of micro sections

The production of a micro section is reduced to the sequential execution of the following operations:

– cutting part of the sample to be examined with the help of electro-spark equipment or an abrasive cutting machine part;

– pressing of the sample in a Bakelite holder, which is carried out on an automatic press for hot pressing;

– direct production of micro sections for metallographic analysis, which is carried out on an automatic grinding and polishing machine and is reduced to the following operations;

– leveling the surface of the cut or fracture by rough grinding;

– fine grinding;

– polishing.

After preparation of the micro section, images of the samples were acquired by scanning electron microscopy (SEM) using a scanning electron microscope "PEM-106I" (Great Britain) equipped with an energy dispersive spectrometer "Oxford".

4. 4. Investigation of the anode capacity of an all-iron flow battery

The experimental setup was based on a previous study [11] and used a flow cell with dimensions of 10 cm^2 (Fig. 1).

A Nafion 115 membrane was used to separate the positive and negative electrolytes. The electrolyte consisted of 1.5 M $FeCl_2$ and 1.5 M NH_4Cl. To ensure the stability of the Fe^{2+}/Fe^{3+} redox couple potential, 0.5 M $FeCl_3$ was added to the positive electrolyte. The positive electrode was made by attaching carbon felt treated with nitric acid to the current collector. Subsequently, it was soaked with methanol for 10 minutes and washed with deionized water.

The charging process involved applying a current with a density of 50 mA/cm^2 until the cell failed or shorted.

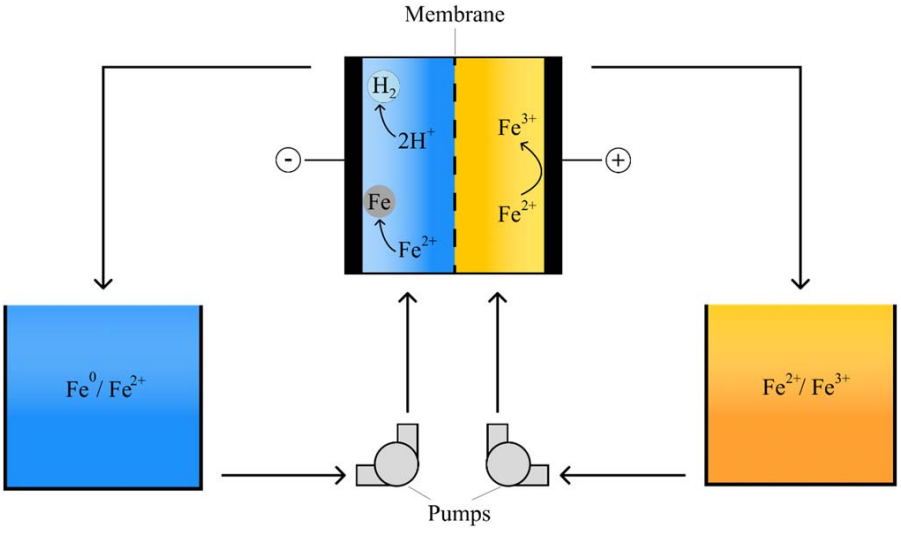

Fig. 1. Schematic representation of an all-iron flow battery [11]

The following configurations of materials were used for different designs of anodes (Fig. 2):

– A – Carbon felt (CF) 2.5 mm thick;

– B – A combination of CF and non-conductive felt (NCF) with a thickness of 1 mm;

– C – Combination of CF and two layers of NCF;

– D – Two layers of CF and one layer of NCF;

– E – Two layers of CF combined with two layers of NCF.

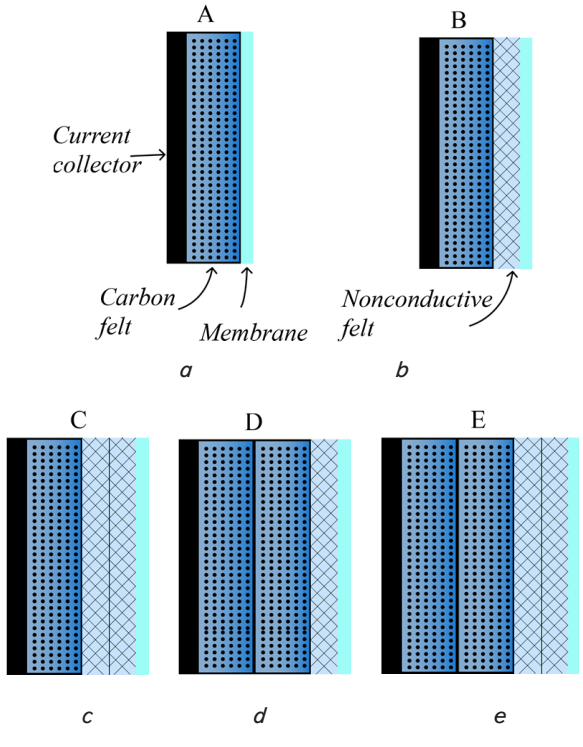

Fig. 2. Schematic representation of the studied electrodes
a – design of the negative electrode of structure A;
b – design of the negative electrode of structure B;
c – design of the negative electrode of structure C;
d – design of the negative electrode of structure D;
e – design of the negative electrode of structure E, tested in an all-iron rechargeable battery

The purpose of the experimental setup was to investigate the capacity and characteristics of various designs of anodes in AIFB. The attention was focused on the assessment of their ability to deposit a uniform layer of iron under the above conditions.

5. Results of investigating the capacity and structure of the all-iron flow battery anode

5. 1. Studying the capacity difference between different anode designs of an all-iron flow battery

Five different negative electrode designs, as shown in Fig. 2, have been thoroughly tested in the context of the AIFB experiment. Hawthorne [11] investigated the process of copper deposition on the negative electrode to minimize the effect of hydrogen evolution as a competing reaction. In order to determine the average charge voltage of AIFB, it was decided to choose iron as the main deposited metal for testing.

All electrode structures (A–E) follow a traditional carbon felt flow architecture, with each felt securely connected to a current collector. Notably, structures B–E include an additional layer of non-conductive felt placed on top of the firmly bonded conductive electrode. The use of porous carbon materials in electrodes (A–E) is strategically important, aimed at minimizing kinetic overvoltage and increasing the mechanical adhesion of the coating. This design choice serves the purpose of increasing efficiency. At the same time, a layer of non-conductive felt serves as a preventive barrier, preventing the direct penetration of iron into the membrane.

Of the five electrode configurations, structures A, B, C, and D failed, falling short of the intended coating capacity limit of 700 mA*h/cm^2. It is noteworthy that structures A–D include only one layer of non-conductive felt, which creates a gap characterized by minimal electronic conductivity. Therefore, the ohmic resistance in these structures depends exclusively on the ionic conductivity.

In comparison, an electrode design including two carbon felts and two layers of non-conductive felt (E) successfully achieved the target iron layer capacity of 700 mA*h/cm^2. The charge profile (Fig. 3) for this particular structure, as well as for those that missed the target, exhibited distinct characteristics.

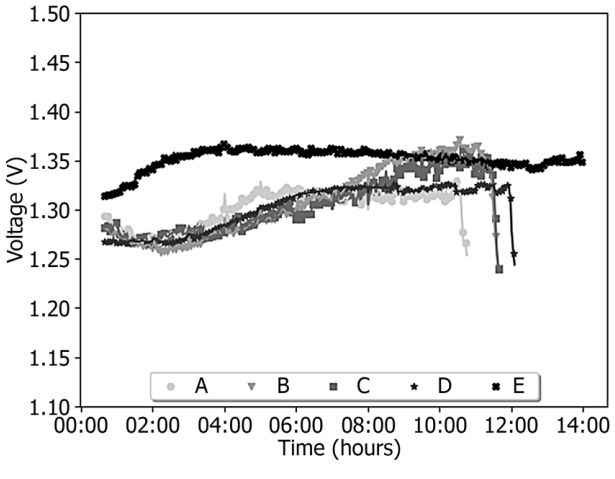

Fig. 3. Charging curves for anode configuration designs of an all-iron flow battery

In particular, the charge potential remained relatively constant for the successful design, in contrast to the rapid spike in potential seen in the failed structures. The results of the average charge voltage and capacity are given in Table 1.

Table 1

Results of electrode capacity testing

Structure	Charge voltage, V	Charge capacity, mAh/cm^2
A	1.303	540
B	1.307	584
C	1.302	583
D	1.298	607
E	1.350	>702

As can be seen from the results, it is obvious that design A exhibits the lowest capacity. Interestingly, structures B and C show similar capacity values, although design C has twice the amount of carbon felt. On the other hand, structures D and E show the highest capacities, with design E outperforming structure D. The main difference between them is the additional layer of non-conductive felt (NCF) in design E. It is noteworthy that these results were obtained with a compression ratio of 80 % for all materials of the negative electrode, which means that the final volume of the anode material in the battery cell occupies 80 % of the initial volume of the material in the free state. This compression ratio (CR) facilitates the distribution of current for the electrode material, which contributes to the deposition of iron on the surface of the electrode due to the lower electrical resistance of the felt compared to the resistance of the electrolyte.

5. 2. Investigation of the distribution of precipitated iron on the surface of electrodes

Photomicrographs were taken of electrode A, D, and E micro sections as these designs were of particular interest due to their excellent lowest and highest capacitance results.

For structure A (Fig. 4), micrographs of the electrode micro section revealed clear areas. The first part showed bare carbon felt (CF) and then a layer of deposited iron on CF. The next part demonstrated a membrane showing significant iron penetration. Finally, a layer of iron was visible on top of the membrane. These observations showed that CF without non-conductive felt (NCF) and with a current compression ratio (CR) of 80 % has a low capacitance, which is exacerbated by the susceptibility of the membrane to iron penetration. The photo of the membrane taken by the camera also shows a thick layer of iron that prevented the membrane from being removed to obtain images of the slices.

For structure D, micrographs of micro sections (Fig. 5) showed three distinct layers. The first layer was bare CF, then CF covered with iron and the next layer of iron on top. A visual inspection of the upper surface of the membrane using a camera showed that iron dendrites occupy approximately 5 % of the electrode surface. In the photomicrograph of the micro sections, the dendrites appeared as a free layer of iron. In this design using 80 % CR, iron deposition was markedly shifted to the surface of the CF, resulting in a high charge capacity (607 mA*h/cm^2) leading to dendritic membrane invasions.

For structure E, which showed the highest capacity, two visible layers are highlighted in the micrographs (Fig. 6). The first layer was uncoated CF, while the second layer contained iron-coated CF. A photograph of the upper surface of the membrane showed the absence of iron dendrites. This is

consistent with the results of the photomicrograph where the deposited iron mainly covers the upper surface of the CF and does not provoke penetration into the membrane.

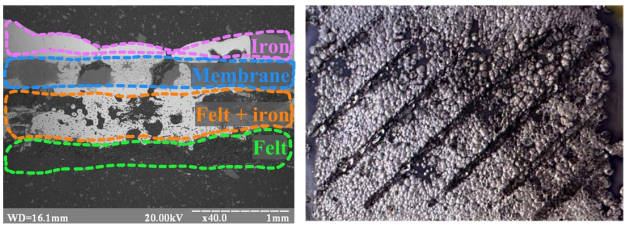

a *b*

Fig. 4. Photographs of the investigated electrode: *a* – microphotograph of a micro section of the electrode section of design A; *b* – photograph of the electrode membrane covered with a layer of iron

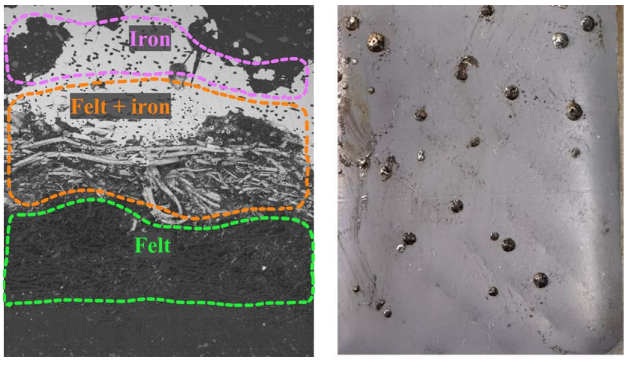

a *b*

Fig. 5. Photographs of the studied electrode: *a* – microphotograph of a micro section of the electrode section of design D; *b* – photograph of the electrode membrane containing iron dendrites

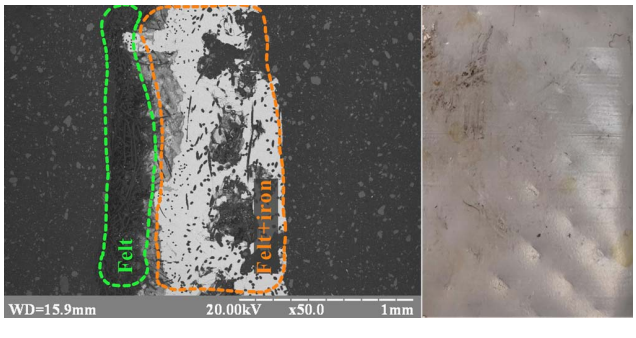

a *b*

Fig. 6. Photographs of the investigated electrode *a* – micrograph of a micro section of the electrode section of design E; *b* – photograph of an electrode membrane with missing dendrites

In summary, the micrographs of micro sections of structures A, D, and E provided valuable information about the nature of iron deposition, emphasizing the critical role of NCF, CR, and the nature of the electrode surface in determining the electrode capacitance and the potential for dendrite formation with subsequent membrane penetration.

5. 3. Examination of the surface of electrodes using scanning electron microscopy and quantitative analysis

When analyzing the SEM images of the surface of the electrodes from the side of the membrane, different characteristics were observed for designs A, D, and E (Fig. 7–9).

In the SEM images of design A (Fig. 7), the surface of CF shows prominent clusters of relatively large iron particles located adjacent to regions of the exposed carbon surface. Observation data indicate the presence of unevenly distributed deposited iron, which indicates suboptimal conditions for iron deposition at a given current density and compression ratio (DC).

For design D, the SEM images (Fig. 8) clearly showed that all carbon felt fibers were uniformly coated with a layer of iron. It is noteworthy that the absence of large iron particles or conglomerates is noticeable. However, similar to design A, there are signs of unevenly distributed deposited iron, which indicates suboptimal conditions for iron deposition at a given current density and CR.

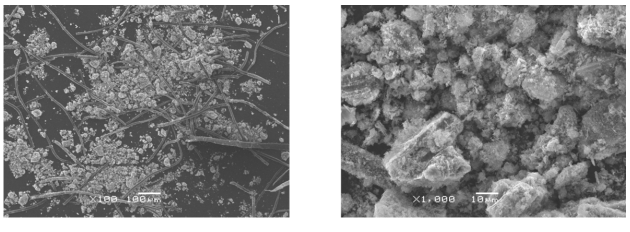

a *b*

Fig. 7. SEM image of the electrode section for design A at different magnifications: *a* – 100x; *b* – 1000x

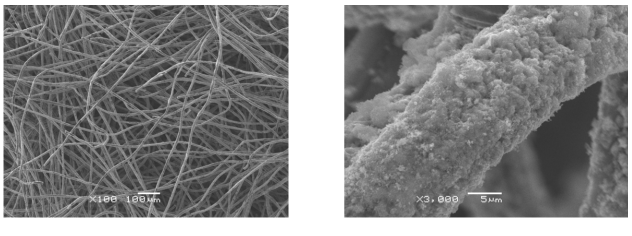

a *b*

Fig. 8. SEM image of the electrode section for design D at different magnifications: *a* – 100x; *b* – 3000x

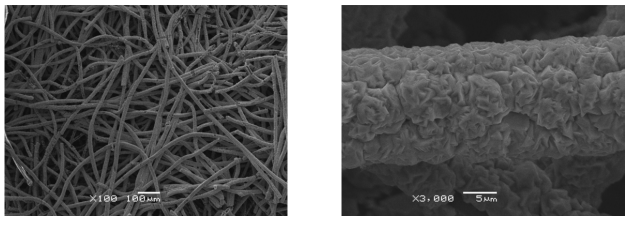

a *b*

Fig. 9. SEM image of the electrode section for design E at different magnifications: *a* – 100x; *b* – 3000x

Design E showed a completely different result (Fig. 9). SEM image revealed that each fiber of the carbon felt was covered with a significant layer of iron without any visible iron particles or conglomerates. In addition, iron deposition was more uniform over the entire surface. This uniform deposition pattern is a strong indication of the improved conditions for iron deposition at the same current density and CR compared to structures A and D.

In conclusion, SEM images of the electrode surface provided visual evidence of the complex interplay between iron deposition, current density, and CR. Design E took the lead by showing uniform iron deposition, suggesting that the combination of these factors was optimal for efficient iron deposition.

SEM images for different sides of electrode E.

Valuable information was obtained during the analysis of SEM images of different sides (from the current collector and from the membrane) of electrode E using quantitative ZAF analysis.

The SEM image (Fig. 10) corresponding to the side of the current collector shows a typical appearance corresponding to the CF material. Rare iron deposits are visible here (approximately 0.42 wt.%), and the deposited iron layer looks relatively thin (Fig. 11).

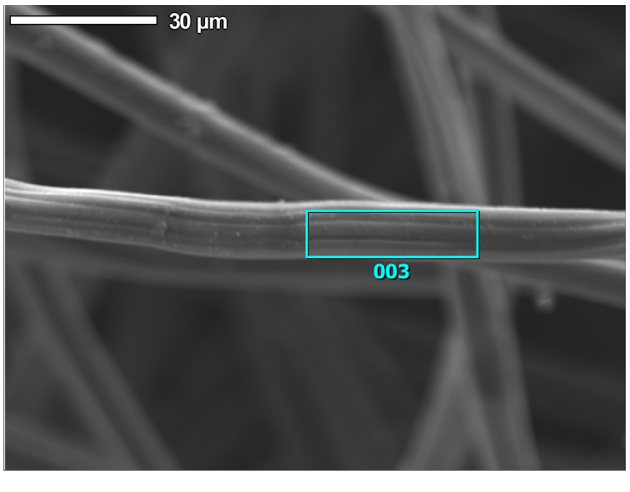

Fig. 10. SEM-image of the surface of the anode of an all-iron flow battery from the side of the current collector

The SEM image (Fig. 12) corresponding to the side of the membrane, on the contrary, shows a clearly different scenario. This side is visibly covered with a significant layer of iron, similar to what is observed in the SEM images

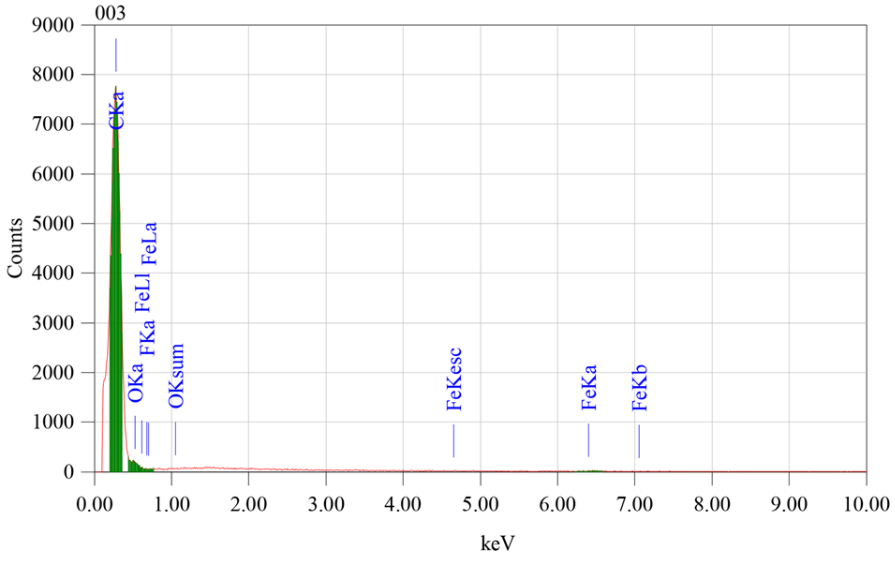

ZAF Method Standardless Quantitative Analysis
Fitting Coefficient : 0.7961

Element	(keV)	mass%	Error%	At%	Compound	mass%	Cation	K
C K	0.277	73.72	0.34	79.08				82.2238
O K	0.525	25.86	3.14	20.83				17.2647
F K								
Fe K	6.398	0.42	9.00	0.10				0.5115
Total		100.00		100.00				

Fig. 11. Quantitative analysis of the anode surface of an all-iron flow battery from the side of the current collector

of electrode E (Fig. 9). It is noteworthy that the layer of deposited iron on this side is much thicker. Quantitative ZAF analysis of the surface showed a mass iron content of 81.67 wt. % (Fig. 13).

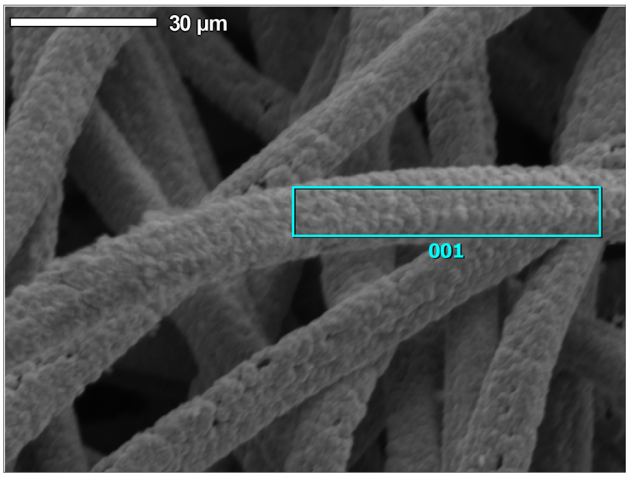

Fig. 12. SEM image of the anode surface of an all-iron flow battery from the side of the membrane

These results emphasize the uniformity of iron deposition on CF at a current density of 50 mA/cm^2 and a compression ratio of 80 %. The uniform deposition strongly indicates that the combination of the above parameters contributed to the optimal deposition of iron. In addition, these findings provide a basis for further determination of the relationships between iron deposition distributions and various electrode designs, considering different current densities and degrees of compression.

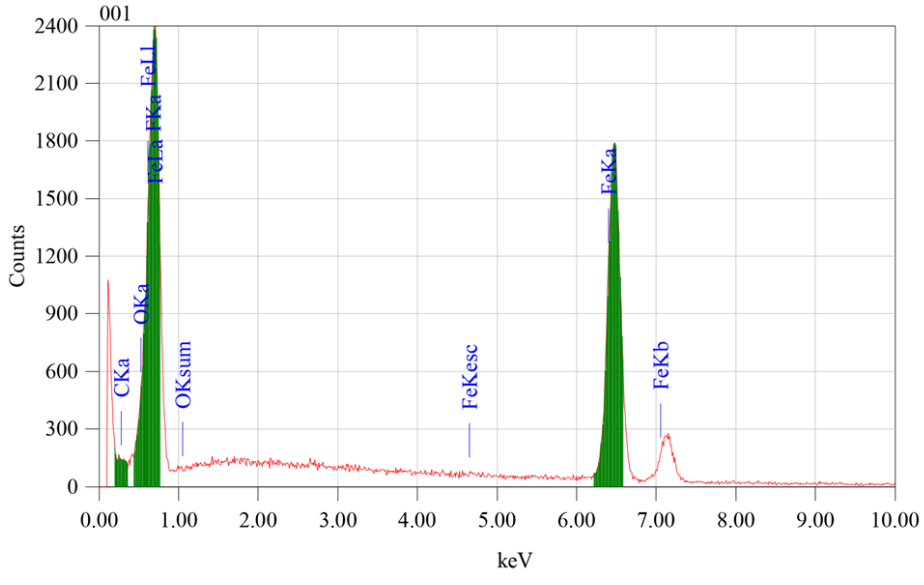

ZAF Method Standardless Quantitative Analysis
Fitting Coefficient : 0.9209

Element	(keV)	mass%	Error%	At%	Compound	mass%	Cation	K
C K	0.277	12.88	1.34	37.93				4.0099
O K	0.525	0.56	1.87	1.24				0.6959
F K	0.677	4.89	1.72	9.11				12.1122
Fe K	6.398	81.67	11.71	51.72				83.1820
Total		100.00		100.00				

Fig. 13. Quantitative analysis of the anode surface of an all-iron flow battery from the side of the membrane

As a result, SEM images combined with quantitative ZAF analysis provided a new perspective on the distribution of iron deposition. The obtained data indicate the need for an in-depth study of the iron deposition model for different electrode designs, current density, and compression ratio.

6. Discussion of results of investigating the anode capacity of an all-iron flow battery

The main aspects of studying the capacitance of the AIFB anode are to determine the influence of different electrode designs on the battery capacity, taking into account the micro- and macrostructural characteristics, the distribution of deposited iron on the surface, as well as the relationship between the capacity and the mechanism of iron deposition.

Our data showed that structures A and B (Table 1) have a lower capacity compared to other designs. This can be explained by the fact that there is less space for iron deposition on the surface of CF electrodes.

In discussing the results for structures C, D, and E, it is important to note that the capacities of these designs are higher. This is especially true of the E structure, which has the highest capacity of all. This confirms the hypothesis that the deposition of iron occurs most on the surface of the electrodes, especially where an additional layer of NCF is used. This provides confirmation that the distribution of iron deposition on the surface determines the capacity of the electrode. Taking into account the results of the study [11] and comparing them with the results of this work, it can be concluded that the addition of an additional layer of NCF significantly increases the capacity of the AIFB anode.

It is also important to note the results of micro- and macrostructural analysis of anodes. Design A (Fig. 4) showed the presence of areas of iron deposition on the surface of CF, but the thickness of the deposited layer is insufficient for high capacity. In the case of design D (Fig. 5), the presence of iron dendrites is observed, which can affect the structural stability of the anode. Design E (Fig. 6), which has the highest capacity, shows a uniform deposition of iron on the surface, which provides high structural stability.

Our study has several strengths. First, it sheds light on the complex relationship between electrode design, deposition pattern, and capacitance in AIFB. By varying the structure and configuration of the negative electrode, valuable information is gained on how different materials and configurations affect capacitance. The current study has an advantage over previous work in that it explores a wider range of design options, improving the understanding of factors affecting battery capacity and performance.

The results obtained in our study address the critical problem of the limited capacity of the negative electrode in hybrid flow batteries, where a metal deposition reaction occurs on one of the electrodes. Owing to the systematic testing of various electrode designs, it was possible to determine configurations that significantly increase the electrode capacity (Table 1). In particular, design E, which contains an additional layer of non-conductive felt, demonstrated the highest capacity, suggesting that it effectively reduces capacity-related limitations. This is due to the increased surface area and optimized iron deposition achieved with this design.

One limitation of this study is that it focuses on a specific set of experimental conditions, including a fixed current density and compression ratio. These conditions may not fully represent all operating scenarios of all-iron flow rechargeable batteries and the results should be interpreted

within these limits. Furthermore, the study was primarily concerned with the capacity and nature of iron deposition, and further research may be needed to understand the long-term stability and effectiveness of these designs in practical applications. The scalability of the proposed solutions should also be studied.

One notable shortcoming of our study is the lack of long-term cycle data, which is crucial for assessing the durability and stability of the identified structures. In addition, the study did not investigate the effect of other operating parameters such as flow rate and temperature, which could affect the performance of AIFB. Future studies should consider these aspects for a comprehensive understanding of the proposed solutions.

The development of this research can cover several directions. First, long-term cycling experiments should be conducted to assess the practical viability of the identified electrode designs. Further optimization of these structures based on scalability, cost-effectiveness, and ease of manufacture should be explored. In addition, the study could be extended to investigate the effect of different operating parameters on efficiency, allowing for a more complete understanding of an all-iron flow battery. Finally, the insights gained from this research can be used to design improved flow batteries with higher capacity and efficiency.

7. Conclusions

1. The capacity variations obtained during the study of five different electrode configurations provided valuable insight into the role of carbon felt (CF) and non-conductive felt (NCF) layers in determining iron deposition efficiency. The electrode design, consisting of two layers of CF and two layers of NCF, demonstrated the highest capacity exceeding 700 mA*h/cm².

2. Studies of the distribution of iron deposition on the surface of the conductive layer of the anode of an all-iron flow battery showed that at a current density of 50 mA/cm^2 and a compression ratio of 80 %, the main amount of deposited iron is concentrated along the surface of the membrane. Therefore, a long time of charging the anode leads to the accumulation of a significant part of the iron and an increase in the risk of its ingrowth into the membrane, which causes the battery cell to short out.

3. SEM analysis of the electrode surface provided a visual analysis of iron distribution and proved the interaction between iron deposition, current density, and CR. Thus, design E demonstrated the most uniform iron deposition. In addition, the best results of iron deposition on CF were achieved at a current density of 50 mA/cm^2 and a compression ratio of 80 %.

Using the quantitative determination of iron deposition by the ZAF correction method, it was determined that the proportion of iron on the surface of contact with the current lead is 0.42 wt. %, at the same time on the surface with the membrane – 81.67 wt. %. These results emphasize the ims portance of uniform deposition of iron over the entire surface of the conductive layer of the electrode.

Conflicts of interest

The authors declare that they have no conflicts of interest in relation to the current study, including financial, personal, authorship, or any other, that could affect the study and the results reported in this paper.

Funding

The study was conducted without financial support.

Data availability

All data are available in the main text of the manuscript.

References

1. 10 Years: Progress to Action (2020). International Renewable Energy Agency (IRENA). Available at: https://www.irena.org/-/media/Files/IRENA/Agency/Publication/2020/Jan/IRENA_10_years_2020.pdf
2. Renewable Power Generation Costs in 2018 (2019). International Renewable Energy Agency (IRENA). Available at: https://www.irena.org/publications/2019/May/Renewable-power-generation-costs-in-2018
3. Gielen, D., Boshell, F., Saygin, D., Bazilian, M. D., Wagner, N., Gorini, R. (2019). The role of renewable energy in the global energy transformation. Energy Strategy Reviews, 24, 38–50. doi: https://doi.org/10.1016/j.esr.2019.01.006
4. Sánchez-Díez, E., Ventosa, E., Guarnieri, M., Trovò, A., Flox, C., Marcilla, R. et al. (2021). Redox flow batteries: Status and perspective towards sustainable stationary energy storage. Journal of Power Sources, 481, 228804. doi: https://doi.org/10.1016/j.jpowsour.2020.228804
5. Zhang, C., Zhang, L., Ding, Y., Peng, S., Guo, X., Zhao, Y. et al. (2018). Progress and prospects of next-generation redox flow batteries. Energy Storage Materials, 15, 324–350. doi: https://doi.org/10.1016/j.ensm.2018.06.008
6. Holland-Cunz, M. V., Cording, F., Friedl, J., Stimming, U. (2018). Redox flow batteries – Concepts and chemistries for cost-effective energy storage. Frontiers in Energy, 12 (2), 198–224. doi: https://doi.org/10.1007/s11708-018-0552-4
7. Ding, Y., Zhang, C., Zhang, L., Zhou, Y., Yu, G. (2018). Molecular engineering of organic electroactive materials for redox flow batteries. Chemical Society Reviews, 47 (1), 69–103. doi: https://doi.org/10.1039/c7cs00569e
8. Zhao, Q., Zhu, Z., Chen, J. (2017). Molecular Engineering with Organic Carbonyl Electrode Materials for Advanced Stationary and Redox Flow Rechargeable Batteries. Advanced Materials, 29 (48). doi: https://doi.org/10.1002/adma.201607007
9. Hruska, L. W., Savinell, R. F. (1981). Investigation of Factors Affecting Performance of the Iron Redox Battery. Journal of The Electrochemical Society, 128 (1), 18–25. doi: https://doi.org/10.1149/1.2127366
10. Noack, J., Wernado, M., Roznyatovskaya, N., Ortner, J., Pinkwart, K. (2020). Studies on Fe/Fe Redox Flow Batteries with Recombination Cell. Journal of The Electrochemical Society, 167 (16), 160527. doi: https://doi.org/10.1149/1945-7111/abcf50

11. Hawthorne, K. L., Petek, T. J., Miller, M. A., Wainright, J. S., Savinell, R. F. (2014). An Investigation into Factors Affecting the Iron Plating Reaction for an All-Iron Flow Battery. Journal of The Electrochemical Society, 162 (1), A108–A113. doi: https://doi.org/10.1149/2.0591501jes
12. Manohar, A. K., Kim, K. M., Plichta, E., Hendrickson, M., Rawlings, S., Narayanan, S. R. (2015). A High Efficiency Iron-Chloride Redox Flow Battery for Large-Scale Energy Storage. Journal of The Electrochemical Society, 163 (1), A5118–A5125. doi: https://doi.org/10.1149/2.0161601jes
13. Dinesh, A., Olivera, S., Venkatesh, K., Santosh, M. S., Priya, M. G., Inamuddin, Asiri, A. M., Muralidhara, H. B. (2018). Iron-based flow batteries to store renewable energies. Environmental Chemistry Letters, 16 (3), 683–694. doi: https://doi.org/10.1007/s10311-018-0709-8
14. Petek, T. J., Hoyt, N. C., Savinell, R. F., Wainright, J. S. (2015). Slurry electrodes for iron plating in an all-iron flow battery. Journal of Power Sources, 294, 620–626. doi: https://doi.org/10.1016/j.jpowsour.2015.06.050
15. Sun, C., Zhang, H., Song, K. (2023). Fe-based redox flow batteries. Reference Module in Chemistry, Molecular Sciences and Chemical Engineering. doi: https://doi.org/10.1016/b978-0-323-96022-9.00020-7